North American pollution outflow and the trapping of convectively lifted pollution by upper-level anticyclone

Qinbin Li,[1] Daniel J. Jacob, Rokjin Park, Yuxuan Wang, Colette L. Heald, Rynda Hudman, and Robert M. Yantosca

Department of Earth and Planetary Sciences, Division of Engineering and Applied Sciences, Harvard University, Cambridge, Massachusetts, USA

Randall V. Martin

Department of Physics and Atmospheric Science, Dalhousie University, Halifax, Nova Scotia, Canada

Mathew Evans

School of the Environment, University of Leeds, Leeds, UK

Received 19 May 2004; revised 12 December 2004; accepted 18 February 2005; published 17 May 2005.

[1] We examine the major outflow pathways for North American pollution to the Atlantic in summer by conducting a 4-year simulation with the GEOS-CHEM global chemical transport model, including a coupled ozone-aerosol simulation with $1° \times 1°$ horizontal resolution for summer 2000. The outflow is driven principally by cyclones tracking eastward across North America at 45–55°N, every 5 days on average. Anthropogenic and fire effluents from western North America are mostly transported north and east, eventually merging with the eastern U.S. pollution outflow to the Atlantic. A semipermanent upper-level anticyclone traps the convective outflow and allows it to age in the upper troposphere over the United States for several days. Rapid ozone production takes place in this outflow, driven in part by anthropogenic and lightning NO_x and in part by HO_x radicals produced from convectively lifted CH_2O that originates from biogenic isoprene. This mechanism could explain ozonesonde observations of elevated ozone in the upper troposphere over the southeastern United States. Asian and European pollution influences in the North American outflow to the Atlantic are found to be dispersed into the background and do not generate distinct plumes. Satellite observations of CO columns from MOPITT and of aerosol optical depths (AODs) from MODIS provide useful mapping of outflow events, despite their restriction to clear-sky scenes.

Citation: Li, Q., D. J. Jacob, R. Park, Y. Wang, C. L. Heald, R. Hudman, R. M. Yantosca, R. V. Martin, and M. Evans (2005), North American pollution outflow and the trapping of convectively lifted pollution by upper-level anticyclone, *J. Geophys. Res.*, *110*, D10301, doi:10.1029/2004JD005039.

1. Introduction

[2] North America is a major source of anthropogenic trace gases and aerosols to the global atmosphere [*Intergovernmental Panel on Climate Change* (*IPCC*), 2001]. The International Consortium on Atmospheric Transport and Transformation (ICARTT) campaign, to be conducted in July–August 2004, will characterize North American chemical outflow through extensive measurements of greenhouse gases, oxidants, aerosols, and their precursors from several aircraft platforms based in the eastern United States. Successful execution of the campaign and interpretation of the data requires an understanding of the pathways and mechanisms for the outflow. We address this issue here with a global three-dimensional (3-D) chemical transport model (CTM) applied to simulations of four past summers (1998, 2000, 2001, 2002) and including an assessment of the value of satellite measurements of CO (MOPITT) and aerosols (MODIS) for observing North American outflow.

[3] Midlatitude cyclones drive most of the outflow from North America to the North Atlantic, even in summer when they are relatively weak [*Dickerson et al.*, 1995; *Merrill and Moody*, 1996; *Moody et al.*, 1996]. The summertime cyclones form in the lee of the Rocky Mountains and along the mid-Atlantic east coast [*Zishka and Smith*, 1980; *Whittaker and Horn*, 1984]. They propagate eastward and poleward before weakening south of Greenland. The associated surface cold fronts sweep southeastward across the eastern United States. There are four basic types of airstreams associated with a midlatitude cyclone: the warm conveyor belt (WCB) ahead of the cold front, the cold conveyor belt (CCB), the dry airstream (DA) subsiding

[1]Now at Jet Propulsion Laboratory, California Institute of Technology, Pasadena, California, USA.

Copyright 2004 by the American Geophysical Union.
0148-0227/05/2004JD005039$09.00

behind the cold front, and the post cold front (PCF) boundary layer airstream [*Carlson*, 1980; *Browning and Monk*, 1982; *Browning and Roberts*, 1994; *Carlson*, 1998; *Cooper et al.*, 2001; *Cooper et al.*, 2002a, 2002b].

[4] Convection has also long been recognized as an effective mechanism for ventilating the continental boundary layer of the United States and providing a direct conduit to the upper troposphere [*Dickerson et al.*, 1987; *Pickering et al.*, 1988, 1992; *Jacob et al.*, 1993; *Thompson et al.*, 1994]. Convection is particularly important for ventilating the southeastern United States in summer, as the WCBs from the midlatitude cyclones generally do not extend that far south. This convective outflow can then remain for several days over the United States in a circulation around a semipermanent upper-level anticyclone, leading to high concentrations of ozone.

[5] In the present work we first conduct a 4-year simulation of carbon monoxide (CO) with the GEOS-CHEM CTM to examine the interannual variability of North American pollution outflow. CO is emitted by incomplete combustion and is also produced within the atmosphere by oxidation of hydrocarbons. It has a lifetime in the atmosphere of about 2 months against oxidation by OH, making it a sensitive tracer for long-range transport of pollution [*Staudt et al.*, 2001; *Liu et al.*, 2003]. We then focus on examining the impact of upper-level anticyclone on convective outflow in the southern United States.

2. Model Description

[6] The GEOS-CHEM CTM is driven by assimilated meteorological data with 6-hour resolution (3-hour for surface variables and mixing depths) from the Goddard Earth Observing System (GEOS-3) of the NASA Data Assimilation Office (DAO). The first description of GEOS-CHEM as applied to simulation of tropospheric ozone-NO_x-hydrocarbon chemistry was presented by *Bey et al.* [2001a]. Other applications have focused on CO [*Duncan et al.*, 2003; *Palmer et al.*, 2003a] and aerosols [*Park et al.*, 2003, 2004; B. N. Duncan et al., Model study of the variability and trends of carbon monoxide (1988–1997): 1. Model formulation, evaluation, and sensitivity, submitted to *Journal of Geophysical Research*, 2005, hereinafter referred to as Duncan et al., submitted manuscript, 2005]. Applications to North American outflow of ozone, CO, and nitrogen oxides were presented by *Li et al.* [2002a, 2002b, 2004]. We use here GEOS-CHEM version 5.04 (available at http://www-as.harvard.edu/chemistry/trop/geos), which includes a simulation of aerosol chemistry coupled to ozone-NO_x-hydrocarbon chemistry [*Park et al.*, 2004].

[7] The GEOS-3 meteorological data are available at $1° \times 1°$ horizontal resolution and 48 σ vertical levels. The boundary layer up to 2 km is resolved by nine layers with midpoints at 10, 45, 115, 220, 370, 580, 870, 1250, and 1740 m altitude for a column based at sea level. We present here global GEOS-CHEM simulations of CO conducted at $2° \times 2.5°$ resolution (i.e., by degrading the meteorological data from $1° \times 1°$ to $2° \times 2.5°$) for the summers of 1998, 2000, 2001, and 2002. We also present a coupled ozone-aerosol full-chemistry simulation at $1° \times 1°$ resolution for the summer of 2000 with a nested model version for North America and the adjacent oceans (10–60°N, 40–140°W) using dynamic boundary conditions from a global $4° \times 5°$ simulation. A detailed description of this one-way nesting in the GEOS-CHEM model is given by *Wang et al.* [2004]. All simulations presented here were conducted for 6 months (March–August) using standard GEOS-CHEM model output as initial conditions. The first 3 months were used for initialization, and we focus our attention on results for June–August.

[8] The model includes over 80 chemical species and 300 reactions to describe tropospheric ozone-NO_x-hydrocarbon-sulfur chemistry. The aerosol simulation is described by *Park et al.* [2003, 2004] and includes sulfate-nitrate-ammonium and carbonaceous aerosols. For sea salt and soil dust aerosols we use monthly mean fields for 1997 from the GOCART CTM [*Ginoux et al.*, 2001; *Chin et al.*, 2002]. Wet deposition of soluble gases and aerosols in GEOS-CHEM is described by *Liu et al.* [2001] and includes scavenging from convective updrafts, rainout from convective anvils, and rainout and washout from large-scale precipitation.

[9] Our CO simulation uses the same CO sources in all 4 years in order to focus on variability in transport. CO sources in the model include fossil fuel and biofuel combustion, biomass burning emissions, and chemical production from atmospheric oxidation of methane, isoprene, and other volatile organic compounds (VOCs). Aseasonal fuel emissions for 1998 are taken from Duncan et al. (submitted manuscript, 2005). Biomass burning emissions are from the *Duncan et al.* [2003] climatology with $1° \times 1°$ spatial resolution and monthly temporal resolution. This climatology includes large forest fires in Canada and the western United States in summer. In the nested simulation for summer 2000, we use specific biomass burning emissions for that year from *Duncan et al.* [2003], again with monthly temporal resolution. Compared with the climatology, the summer of 2000 had few boreal forest fires in Canada but large forest fires in the northwestern United States in July and August.

[10] The major sink for CO is reaction with OH. The CO-only simulations presented here use archived OH fields from a full chemistry simulation, as was done previously by *Bey et al.* [2001b]. To identify source regions and types contributing to the North American outflow, we transport separately in the model a suite of CO tracers, i.e., "tagging" emissions from different source regions and types, a technique that has been used previously in a number of GEOS-CHEM applications [*Bey et al.*, 2001b; *Li et al.*, 2002a; *Liu et al.*, 2003]. We use here four geographical tracers for anthropogenic emissions (North America, Asia, Europe, and the rest of the world) and two for biomass burning (North America and the rest of the world). Since our simulation of CO is linear, the sum of the separate tracers is close to the total simulated CO concentrations, not exactly so because of small nonlinearities in transport.

3. Observations

[11] We will compare here the GEOS-CHEM fields to CO columns from MOPITT and to AODs from MODIS and from the AERONET network. Both MOPITT and MODIS are aboard the Terra satellite in Sun-synchronous polar orbit with 1030 local time overpass (another MODIS instrument

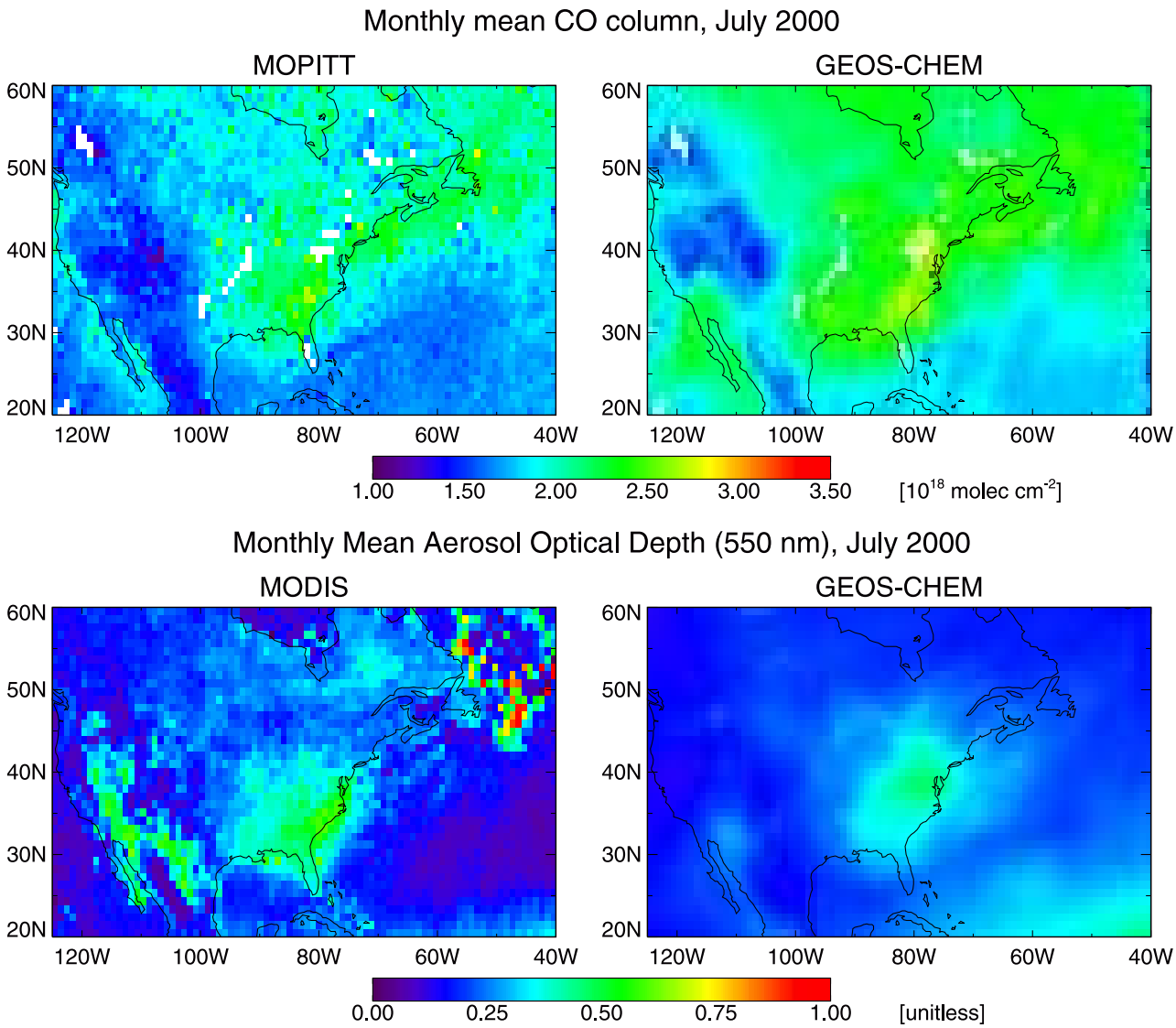

Figure 1. Monthly mean CO columns from MOPITT and aerosol optical depths at 550 nm from MODIS for July 2000. White areas indicate missing data. Corresponding GEOS-CHEM model results are on the right. The observations are at 1030 local time and model results are sampled at 0900–1200 local time. MOPITT data are available for 1–3, 15–31 July only. GEOS-CHEM results for comparison with MOPITT are sampled along the MOPITT orbit tracks, for scenes with successful retrievals, and are processed with the local MOPITT averaging kernels as described by *Heald et al.* [2003].

is on board the Aqua satellite but those data were not used here). MOPITT observes the infrared emission of CO in the nadir and obtains 1–2 pieces of information on the vertical profile weighted toward the middle and upper troposphere [*Deeter et al.*, 2003; *Heald et al.*, 2003]. Previous comparisons of GEOS-CHEM to MOPITT were presented by *Heald et al.* [2003] in a study of Asian outflow and transpacific transport of pollution and by *Arellano et al.* [2004] in a global inverse analysis of CO sources. For comparison with MOPITT, we sample GEOS-CHEM along the satellite orbit track and only for scenes with successful retrievals (clear skies). Following *Heald et al.* [2003], we focus on the column CO data and apply the MOPITT averaging kernels for the individual retrievals to the GEOS-CHEM vertical profiles. Figure 1 (top) shows observed and simulated monthly mean CO columns for July 2000. Elevated CO columns are seen in the eastern United States and downwind over the North Atlantic.

[12] Simulated CO columns are 14% too high relative to MOPITT values, particularly over the source regions such as the Middle Atlantic states, the Gulf Coast, and the Los Angeles Basin and downwind of these source regions (Figure 2). Comparison of MOPITT and model simulated vertical profiles over the region defined by 75°–85°W, 40°–45°N (Maryland, Delaware, New Jersey, and Pennsylvania), where the discrepancy is largest, shows that model simulated CO concentrations are higher by 20–40 ppb than MOPITT retrievals. This discrepancy may partly be explained by the relatively low sensitivity of MOPITT in the lower tropoposphere, particularly in the boundary [*Heald et al.*, 2003]. Applying the MOPITT averaging kernel bringing model simulated boundary layer

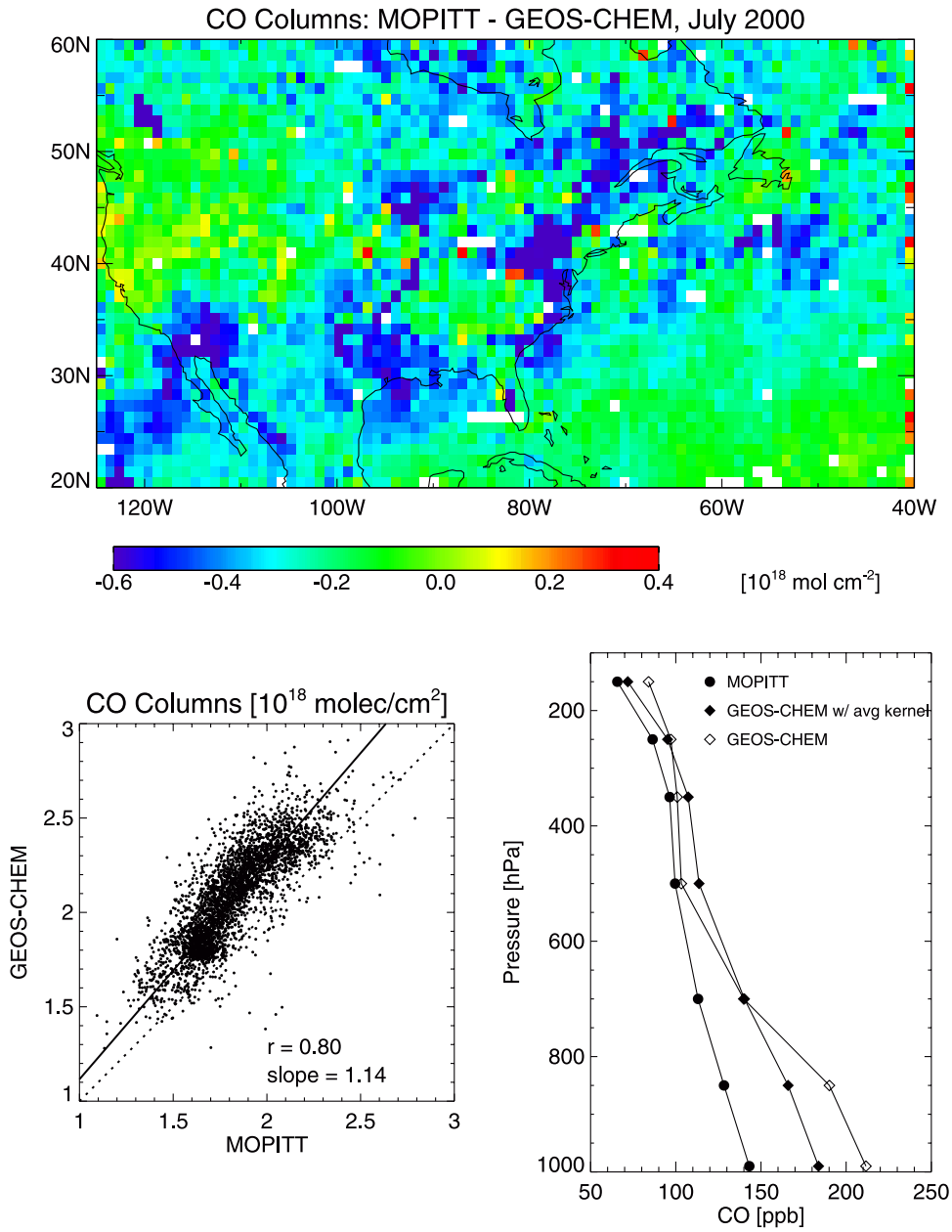

Figure 2. Difference between MOPITT and GEOS-CHEM simulated monthly mean CO columns July 2000. White areas indicate missing data. Bottom left shows scatterplot of MOPITT and model CO columns. Bottom right shows averaged CO vertical profiles over 75°–85°W, 40°–45°N.

CO concentrations by 20–25 ppb, as shown in Figure 1. Considering that we used 1998 emissions for all the model simulations presented here, the discrepancy could also be partly explained by the difference in CO emissions between 1998 and 2000. Emission trends data from the U.S. Environmental Protection Agency indicate a 5% per year average annual decrease in CO vehicular emissions [*United States Environmental Protection Agency*, 2000; *Parrish et al.*, 2002].

[13] MODIS uses observations of solar backscatter in seven spectral channels (470–2100 nm) for its AOD retrieval [*Kaufman et al.*, 1997; *Tanré et al.*, 1997]. Validation with the AERONET surface network indicates retrieval errors of $\Delta AOD = \pm 0.05 \pm 0.2AOD$ over land [*Chu et al.*, 2002] and of $\Delta AOD = \pm 0.03 \pm 0.05AOD$ over ocean [*Remer et al.*, 2002]. Since MODIS provides about 95% coverage of the Earth in a day [*Chu et al.*, 2003], we do not attempt to resolve orbit tracks and simply sample the model globally for that particular day at 0900–1200 local time. We calculate the AOD in GEOS-CHEM from the mass concentration and extinction efficiency for each aerosol type following *Martin et al.* [2003]. Aerosol properties assumed in the model may be different from those assumed in the MODIS retrieval, but we do not attempt to take into account this difference. Figure 1 (bottom) shows observed and simulated monthly mean AODs (at 550 nm) for July 2000. Elevated AODs are seen over the eastern United States. The weaker pollution

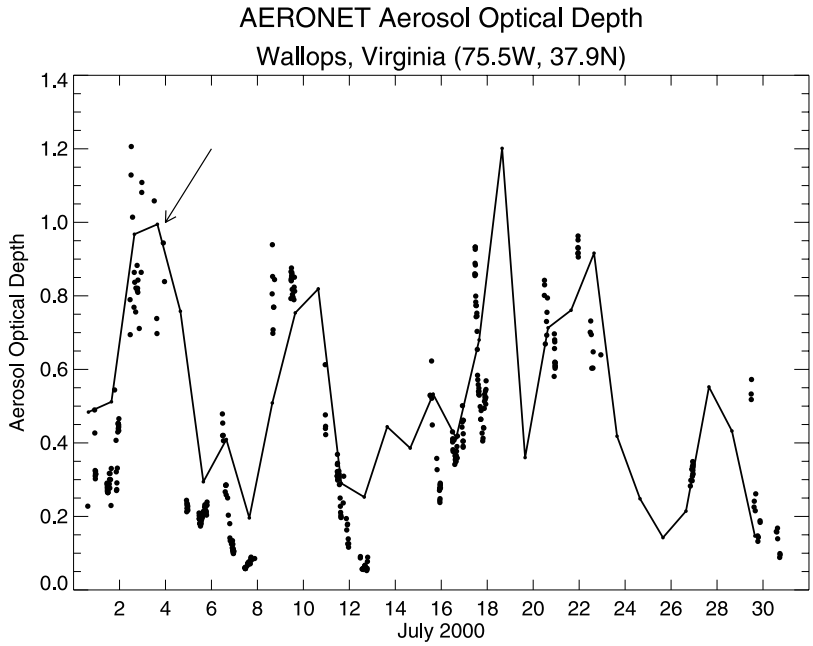

Figure 3. Aerosol optical depths (at 440 nm) at Wallops, Virginia (75.5°W, 37.9°N) for July 2000. The dots are AERONET observations (from http://aeronet.gsfc.nasa.gov) and the solid line is GEOS-CHEM average over 0900–1200 local time. The arrow indicates the pollution episode discussed in the text.

influence over the North Atlantic as compared with MOPITT reflects scavenging of aerosols. The unusually high values east of Newfoundland are likely due to cloud contamination. Dusty regions of the western United States, where MODIS also observes high values, are known to be subject to large retrieval errors [*Chu et al.*, 2003].

[14] Sites of the AERONET network make direct solar radiation measurements at 340–1020 nm wavelengths with Sun-sky scanning spectral radiometers [*Holben et al.*, 1998]. We use here AODs reported at 440 nm. Figure 3 compares simulated versus observed time series of AERONET AODs at Wallops Island, Virginia (75.5°W, 37.9°N). Model values are also for 440 nm and are averages for 0900–1200 local time. The model captures the major pollution episodes seen in the observations; the arrow indicates a specific event to be discussed in the text.

4. North American Outflow Pathways

4.1. Meteorological Setting

[15] Summertime cyclones over North America are generally located farther north than their cold-season counterparts and are less frequent. The summer maximum of cyclone activity is between 45°N and 55°N, with the maximum frequency found in the James Bay area of Canada and off the Labrador coast [*Zishka and Smith*, 1980; *Whittaker and Horn*, 1984]. The cyclones form in the lee of the Rocky Mountains and over the mid-Atlantic coast of the United States. There are four main cyclone tracks: two across central Canada merging over James Bay, one across the northern United States, and a fourth along the mid-Atlantic coast. As the cyclones track northeastward, the associated surface cold fronts sweep southeastward across eastern North America. South of 35°N, the cold fronts often become stationary and dissipate as the temperature contrast across the front decreases. As a result, the WCBs associated with the cold fronts generally originate in the central United States [*Stohl*, 2001; *Eckhardt and Stohl*, 2004] and extend northeastward, ending in the upper troposphere over the Canadian Maritime Provinces and Newfoundland.

[16] Figure 4 shows GEOS-3 winds at 950 hPa and 500 hPa for July of the 4 simulation years. At 950 hPa winds are weak and disorganized over the eastern United States. Northwesterly flow prevails from Manitoba to the Great Lakes and the northeast coast, strongest in 1998, while southwesterly flow prevails from the northeast coast to the Canadian Maritime Provinces and Newfoundland. A prominent feature of the circulation over the United States is the strong low-level jet transporting air and moisture from the Gulf of Mexico to the central United States up to about 45°N, weakest in 2002. The low-level jet and the surface heat low in summer lead to convergence and convection in the central United States, resulting in frequent occurrence of mesoscale convective complexes (MCCs) [*Maddox*, 1980].

[17] At 500 hPa, a strong anticyclone dominates the south-central and southwestern United States. Previous climatological analyses have shown that this anticyclone is semipermanent in summer due to intense surface heating [*Bell and Bosart*, 1989; *Parker et al.*, 1989]. It only occasionally breaks open. As will be discussed in section 5, this anticyclonic circulation has important implications for the fate of convective outflow over the United States. The anticyclone, the strong upper-level Hudson Bay Low, and the northward expansion of the subtropical Bermuda high result in a wave-like flow pattern at 500 hPa. Northwesterly flow prevails from Manitoba to the northeast coast, while southwesterly flow dominates from the northeast coast to the Canadian

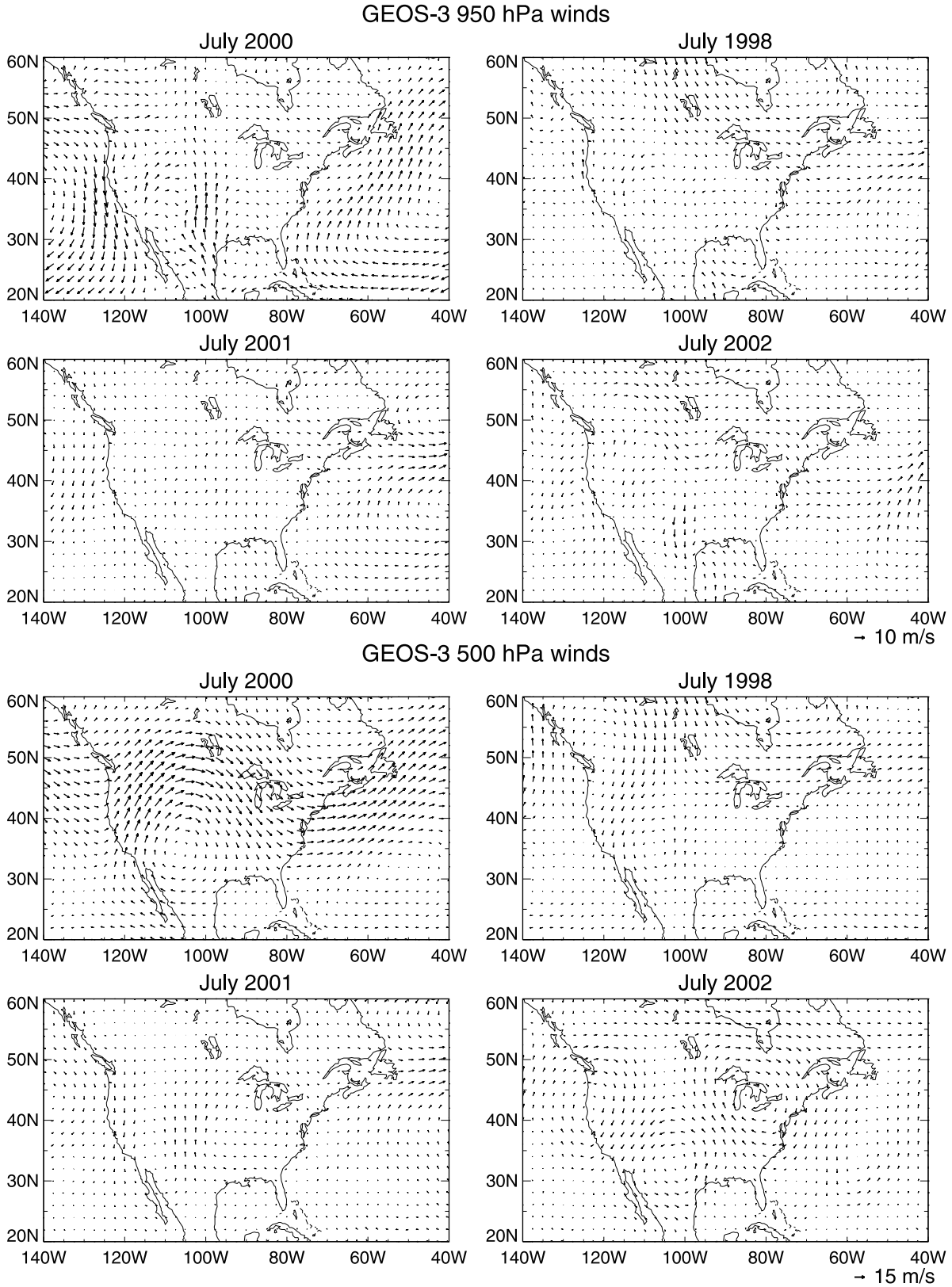

Figure 4. Monthly mean GEOS-3 winds at 950 hPa and 500 hPa for July 2000 and the differences relative to July 2000 for 1998, 2001, and 2002.

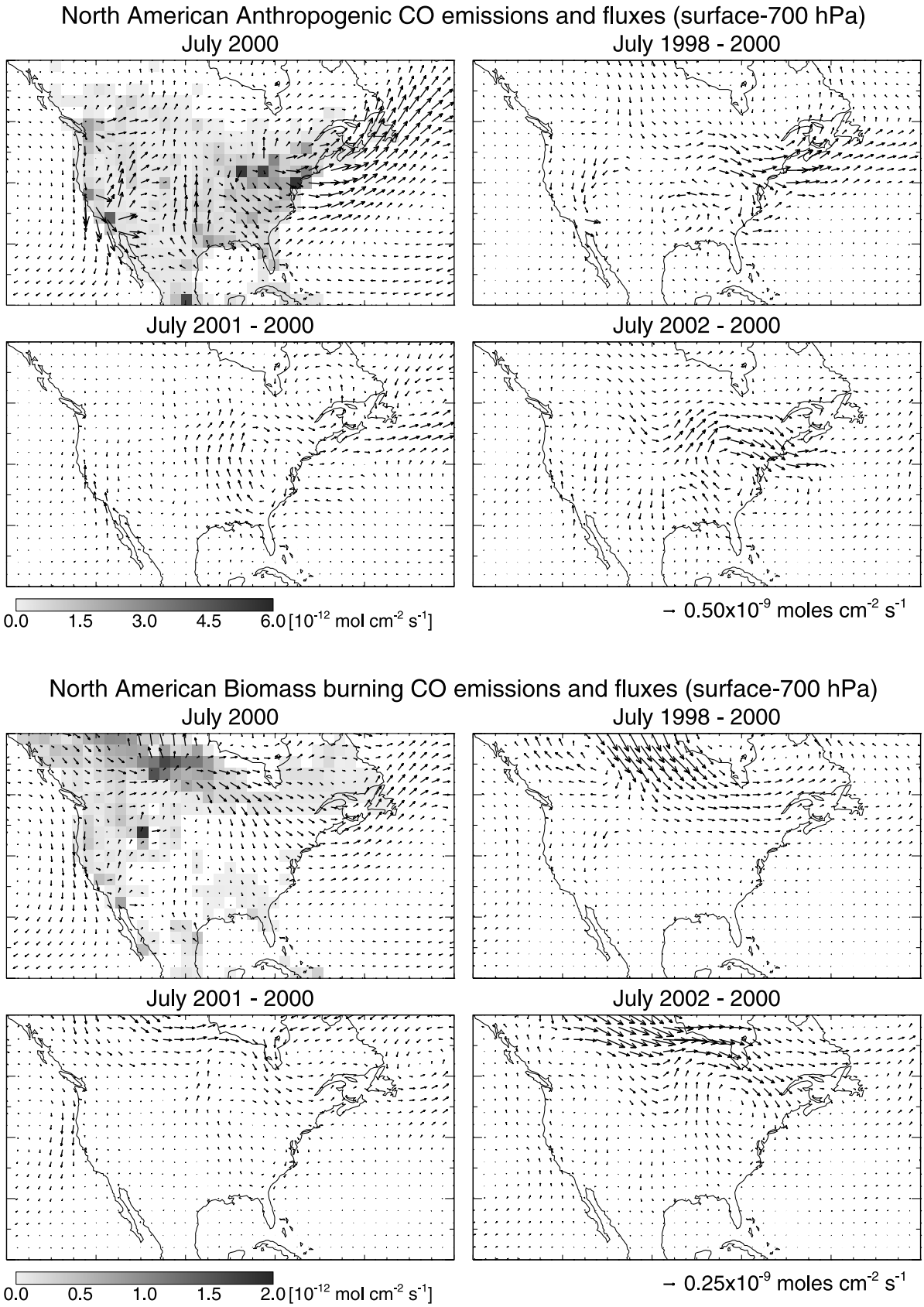
North American Anthropogenic CO emissions and fluxes (surface-700 hPa)
July 2000
July 1998 - 2000
July 2001 - 2000
July 2002 - 2000
0.0 1.5 3.0 4.5 6.0 [10^-12 mol cm^-2 s^-1]
→ 0.50x10^-9 moles cm^-2 s^-1
North American Biomass burning CO emissions and fluxes (surface-700 hPa)
July 2000
July 1998 - 2000
July 2001 - 2000
July 2002 - 2000
0.0 0.5 1.0 1.5 2.0 [10^-12 mol cm^-2 s^-1]
→ 0.25x10^-9 moles cm^-2 s^-1

Figure 5

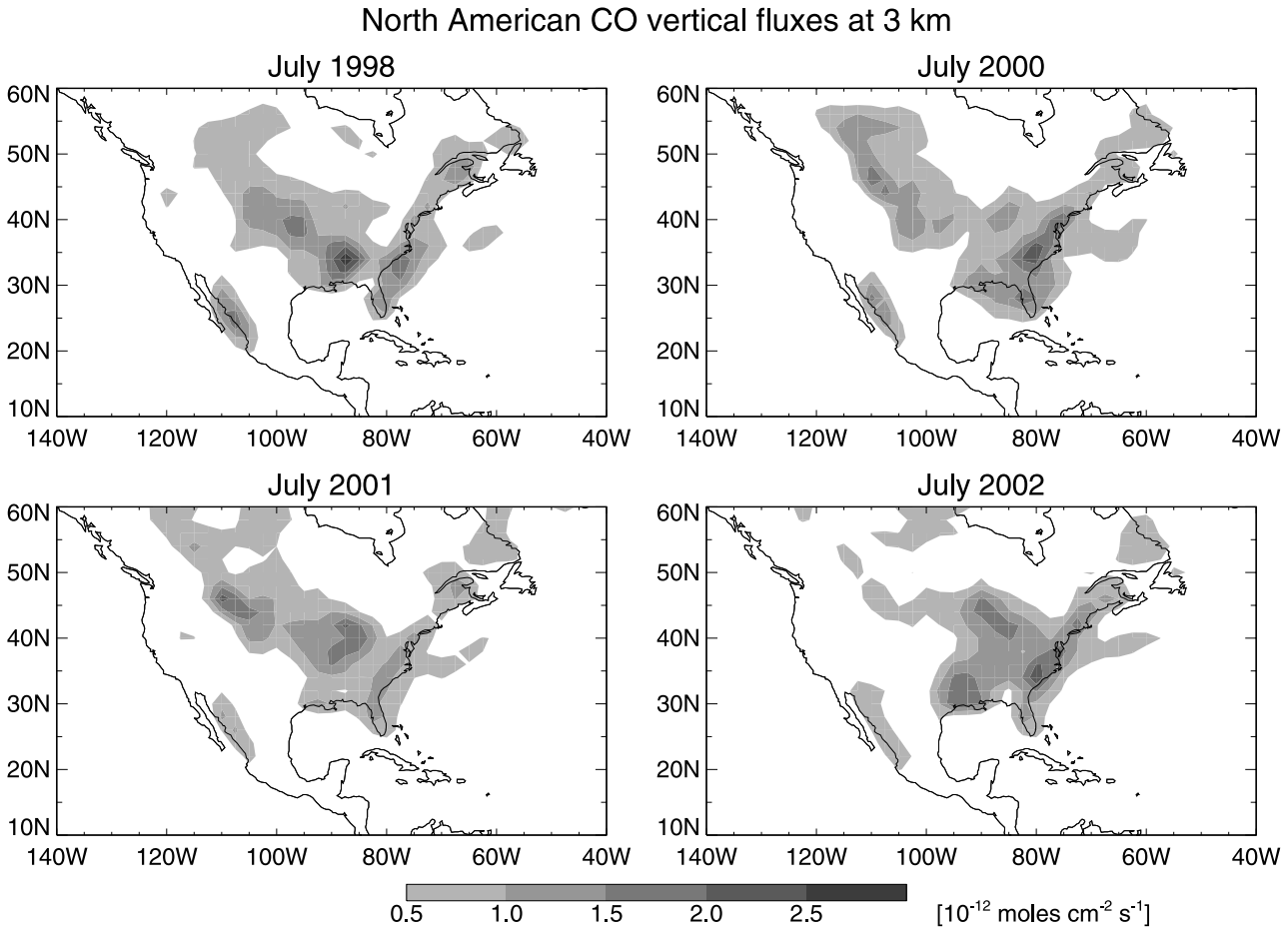

Figure 6. GEOS-CHEM monthly mean vertical fluxes of North American CO at 3 km for July 1998, 2000, 2001, and 2002.

Maritime Provinces and Newfoundland. The maximum winds across the east coast are further south in 2000 and 2001 than in 1998 and 2002. Flow patterns at 300 hPa are similar to those at 500 hPa and are not shown here. The anticyclonic circulation is also evident at 300 hPa.

4.2. Interannual Variability of North American Outflow

[18] Figure 5 shows July monthly mean horizontal fluxes of North American anthropogenic and biomass burning CO averaged over the 1000–700 hPa column for the 4 simulation years. These fluxes were calculated from the tagged CO tracer simulation (section 2). Strong CO fluxes across the east coast of North America span a wide latitude range between 30°N and 55°N, consistent with a previous study of North American outflow to the North Atlantic by *Whelpdale et al.* [1984]. The northeastern United States, the Canadian Maritime Provinces, and Newfoundland are heavily influenced by anthropogenic outflow, which is strongest in 1998 and 2002 and weakest in 2001, reflecting the different strength of the respective winds (Figure 4). Biomass burning CO, mainly emitted in boreal Canada and the northwestern United States in summer, is transported first southeastward to the Great Lakes region and the northeast United States and then northeastward to the Canadian Maritime Provinces and Newfoundland. Biomass burning influence reaches the southeast United States in July 2000 and 1998 but not significantly in the other 2 years. Previous studies have shown that Canadian forest fire emissions can cause major enhancements of CO and aerosols in the southeastern United States in summer [*Wotawa and Trainer*, 2000; *Park et al.*, 2003; *Lamarque et al.*, 2003]. Biomass burning outflow is strongest in 1998 and 2002.

[19] The West Coast of the United States is a major anthropogenic source. The main export route from this region is northward to 45–50°N, then eastward to the midwest, and eventually merging with the east coast pollution outflow. About half of this export takes place in the free

Figure 5. GEOS-CHEM monthly mean horizontal fluxes of North American anthropogenic and biomass burning CO averaged over the 1000–700 hPa column for July 2000 and the difference relative to July 2000 for 1998, 2001, and 2002."North American CO" refers to CO originating from anthropogenic and biomass burning emissions over North American continent. Also shown are anthropogenic and biomass burning CO emissions. Anthropogenic emissions from 1998 and climatological biomass burning emissions are used for all 4 years so that flux differences are due to meterology. Note the difference in arrow scales for the anthropogenic and biomass burning parts.

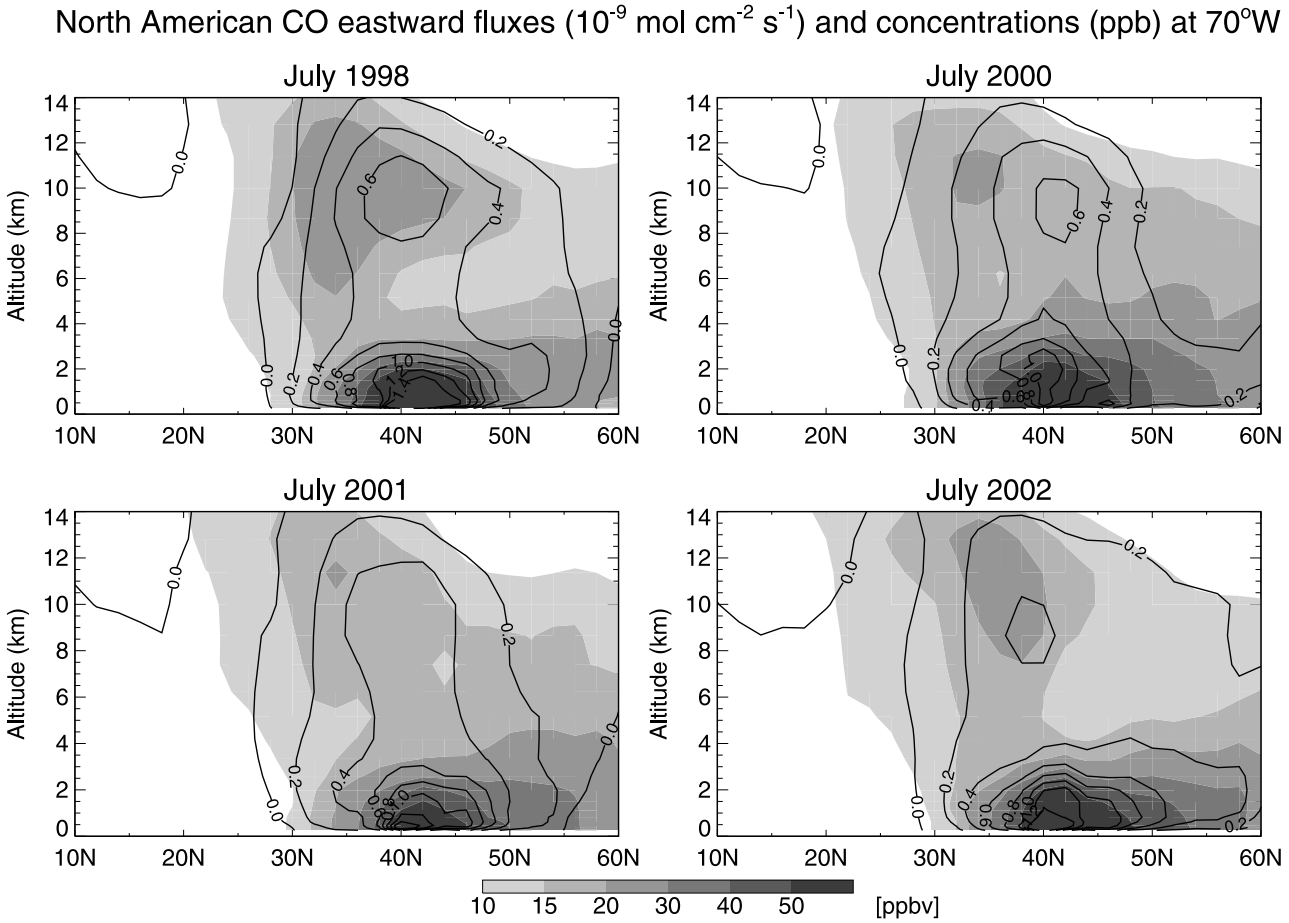

Figure 7. GEOS-CHEM monthly mean zonal fluxes (line contours) and concentrations (color contours) of North American CO at 70°W for July 1998, 2000, 2001, and 2002.

troposphere above 3 km. Only a small fraction of the West Coast pollution is exported southwest to the Pacific where it enters the large-scale transport around the Pacific High. The latter mechanism is known to cause events of long-range transport of North American pollution to Hawaii in summer [*Galasyn et al.*, 1987; *Moxim*, 1990; *Balkanski et al.*, 1992], but it is in fact only a minor outflow pathway. Pollution from the Gulf coast and Texas is similarly transported to 45–50°N by the low-level jet followed by eastward transport to the Great Lakes region and the northeast United States, merging there with the east coast outflow. This is an important export route for the Gulf Coast pollution in addition to convective outflow.

[20] Figure 6 shows mean North American CO vertical fluxes at 3 km in July for the four simulation years. Here North American CO refers to CO originating from both anthropogenic and biomass burning emissions over the continent. Deep convection is most active over the Midwest, the Gulf Coast, and the east coast. It lifts surface pollution to the upper troposphere from where it is generally transported northeastward. However, we find that surface pollution convected to the upper troposphere over the central and southeast United States tends to circulate around the upper-level southwestern U.S. anticyclone (Figure 4, bottom) and can age for several days over the United States, as will be further discussed in section 5.

[21] Figure 7 shows the simulated latitude-altitude cross section at 70°W (roughly along the east coast) of monthly mean concentrations and eastward fluxes of North American CO for July. In all 4 years, North American pollution influence is strongest at 35°–50°N in the boundary layer and at 30°–40°N in the upper troposphere. The tagged

Table 1. North American Outflow of CO Across 70°W Longitude in July[a]

Altitude	1998	2000	2001	2002
0–3 km				
Anthropogenic	0.285 (3.44)	0.229 (2.76)	0.186 (2.25)	0.280 (3.38)
Biomass burning	0.090 (1.08)	0.070 (0.84)	0.066 (0.80)	0.100 (1.21)
3–8 km	0.137 (3.17)	0.133 (3.06)	0.123 (2.83)	0.137 (3.17)
8–15 km	0.119 (3.65)	0.101 (3.08)	0.099 (3.03)	0.104 (3.18)

[a]Results are monthly averages at 30°–60°N along 70°W longitude. Values given in units of mol cm^2 s^{-1}. Values in parentheses are outflow in units of Tg CO.

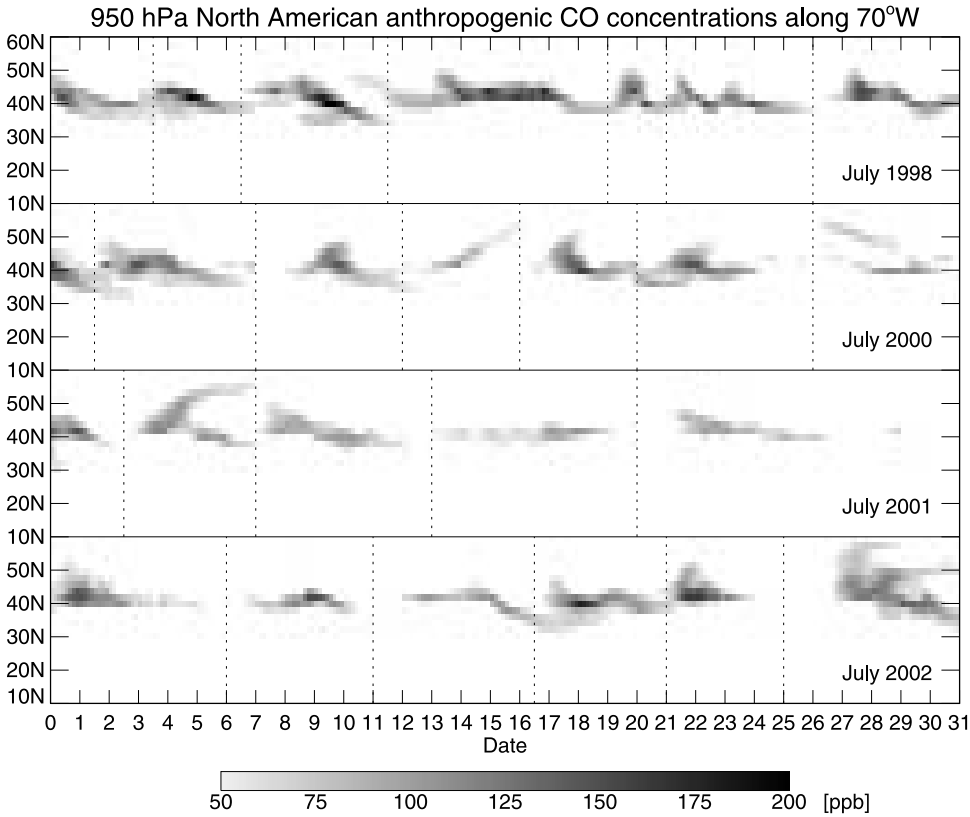

Figure 8. Time series of GEOS-CHEM simulated North American anthropogenic CO concentrations at 950 hPa along 70°W for July 1998, 2000, 2001, and 2002. Values below 50 ppb are not shown. The dashed lines separate the different outflow events.

tracer simulations show that both reflect anthropogenic emissions. The same simulations also indicate that biomass burning influence is strongest at 40°–55°N in the boundary layer. Case studies have shown that smoke from large fires can be injected to altitudes as high as 15 km by supercell convection[*Fromm and Servranckx*, 2003]. Data on forest fire plume heights, not yet available, are required for a more realistic simulation of biomass burning emission influence. Table 1 compares the strength of North American CO outflow in the 4 simulation years. Outflow is strongest in 1998 both in the boundary layer and in the free troposphere and weakest in 2001. North American CO outflow in the boundary layer accounts for 33%, 31%, 28%, and 35% of the total eastward export.

[22] We also compared the frequency and intensity of North American outflow events in July of the 4 simulation years by examining time series of North American CO concentrations along the east coast. Figure 8 shows time series of simulated 950 hPa North American anthropogenic CO concentrations at 10°–60°N along 70°W longitude. Again, North American outflows are concentrated at 35°–50°N. The frequency of North American outflow events (defined here as North American anthropogenic CO larger than 50 ppb) is five to seven, typical for July of the 4 years. The outflow events in July 2000 as indicated by CO concentrations correspond very well with outflow events indicated by the AODs observed at Wallops (Figure 3). Outflow is most frequent and strongest in 1998 among the 4 years with seven events and highest CO enhancements. Outflow is least frequent and weakest in 2001. Examination of time series of 300 hPa North American CO concentrations indicate that convective outflow is also strongest in 1998 and weakest in 2001 (not shown here).

4.3. Episodic North American Outflow

[23] Export from North America is highly episodic, associated with the passage of cold fronts and convective activity [*Cooper et al.*, 2001]. We find 21 outflow events associated with frontal passages during the summer of 2000, for a mean recurring frequency of every 4 to 5 days. We find that the most typical North American outflow pattern in summer is associated with cyclones tracking from the Great Lakes region to Newfoundland and the associated surface cold fronts sweeping across the northeastern United States. Here we illustrate one such event that took place on 3–6 July and terminated a regional pollution episode.

[24] Pollution episodes in the eastern United States are associated with weak anticylones [*Logan*, 1989], and such were the conditions on the days preceding 3 July. The pollution episode over the east coast is indicated by the elevated CO columns on 2–3 July (Figure 9, top). Enhanced CO columns are seen over and to the east of Newfoundland due to a previous outflow event. On 4 July the high pressure over the eastern United States began to give way as low pressure forming over James Bay moved southeastward. The low intensified into a cyclone and the associated surface cold front swept southeastward across the northeastern United States. On 5 July the cyclone was

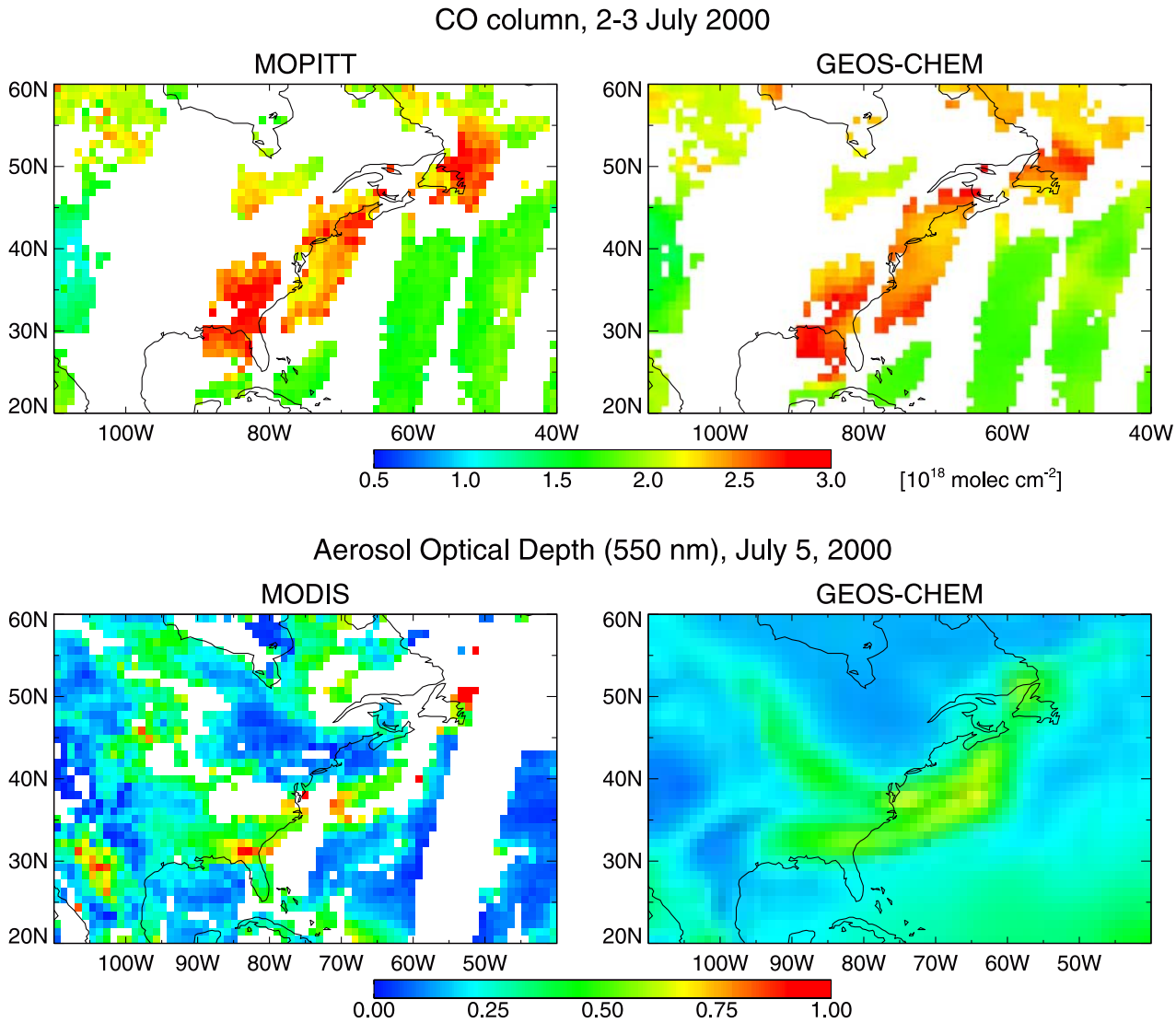

Figure 9. Composite maps of CO columns for 2–3 July 2000 from MOPITT and aerosol optical depths (at 550 nm) for 5 July 2000 from MODIS. Corresponding GEOS-CHEM results are shown at the right.

located over the Gulf of St. Lawrence, where the WCB reached its highest altitude.

[25] Figure 10 shows simulated CO concentrations at 950 on 5 July. The sharp change in the direction of the 950 hPa wind indicates the location of the surface cold front. There was WCB outflow ahead of and boundary layer outflow behind the surface front. High AODs were seen by MODIS in the boundary layer outflow (Figure 9, bottom). MODIS does not provide aerosol data in regions covered by clouds, but model AODs indicate transport in the WCB at 33–37°N along the east coast. AERONET AODs at Wallops, Virginia increased from 0.2 on 2 July to over 0.8 on 3 July during the pollution episode and decreased back to 0.2 on 5–6 July (Figure 3) as the cold front passed through.

[26] We find that boundary layer outflow is capped below 3 km altitude, with highest concentrations reaching 240, 90, and 5 ppb below 2 km for CO, ozone, and sulfate, respectively. The WCB outflow reached 8–10 km altitude in the upper troposphere over the Gulf of St. Lawrence, where ozone concentrations are still elevated (80 ppb) while sulfate is depleted. A subsiding tongue of high ozone from the upper troposphere is seen behind the cold front, reaching down to 4 km, associated with the dry intrusion behind the cold front [*Cooper et al.*, 2001; *Cooper et al.*, 2002a].

5. Anticyclonic Circulation of Convective Outflow in the Upper Troposphere

[27] In summer, and particularly in July and August, the upper-level flow over the southern United States is dominated by a semipermanent subtropical anticyclone (section 4.1). Convective outflow to the upper troposphere, as frequently occurs over the central and southeastern United States in summer (Figure 6), can circulate around this anticyclone for several days. Figure 11 shows the GEOS-CHEM monthly mean horizontal flux of North American anthropogenic CO averaged over the upper tropospheric 400–150 hPa column for July 2000. Circulation of pollution around the upper-level anticyclone is

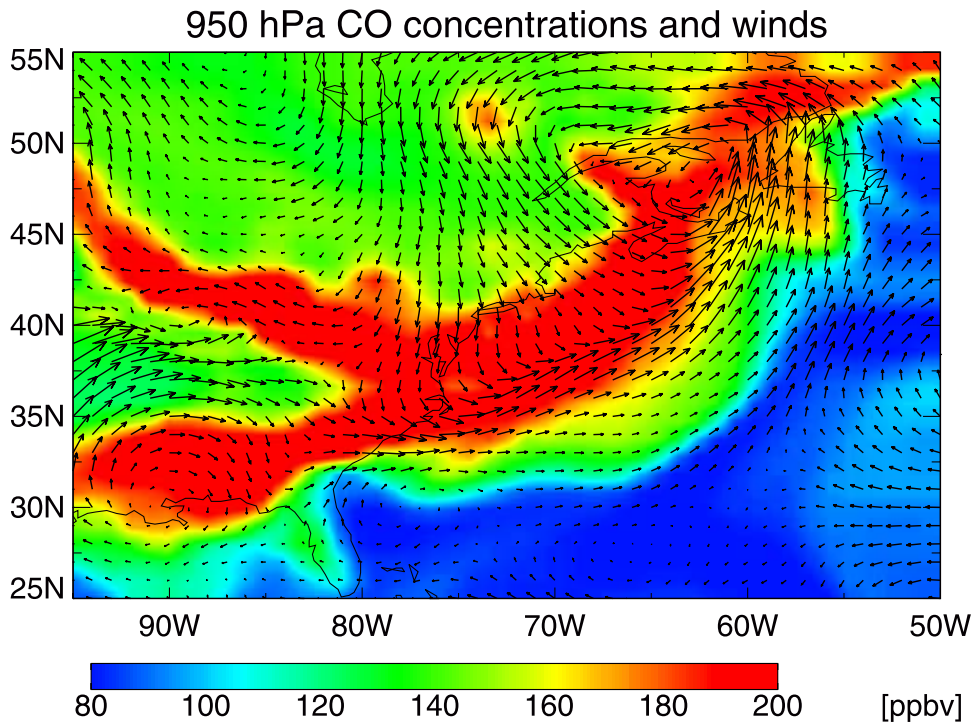

Figure 10. GEOS-CHEM simulated CO concentrations at 950 hPa and winds at 12 GMT on 5 July 2000.

evident and has important implications for chemical aging, in particular ozone production.

[28] Figure 12 shows simulated monthly mean CO and ozone concentrations at 300 hPa for July 2000. The CO maximum over the Gulf Coast corresponds to a region of strong deep convection (Figure 6). Biogenic isoprene emissions are also high in this region [*Palmer et al.*, 2003b] and make a dominant contribution to the CO enhancement (Figure 12). The ozone maximum is shifted to the west over Texas relative to CO, reflecting production in the upper troposphere during circulation around the anticyclone. Also shown in Figure 12 are the simulated enhancements of CO and ozone at 300 hPa from North American anthropogenic, biogenic, and lightning emissions, as determined by difference with sensitivity simulations where these emissions are shut off separately. We see that the ozone enhancement is mostly anthropogenic; about 75% of this anthropogenic contribution is due to production in the lower troposphere followed by convective pumping, with the remainder produced in the upper troposphere. Biogenic and lightning emissions also make significant contributions to the ozone enhancement, mainly by production in the upper troposphere as discussed further below, and are responsible for the westerly shift of the ozone maximum. Stratospheric influence contributes up to 10 ppb ozone over Texas, reflecting subsidence associated with the upper-level anticyclone. Overall, the combination of factors contributing to this ozone maximum are remarkably similar to that we previously discussed as responsible for the upper tropospheric ozone maximum over the Middle East in summer [*Li et al.*, 2001]. Both are found in upper-level anticyclones downwind of deep convective regions with high emissions of anthropogenic precursors.

[29] Figure 13 shows the simulated net ozone production rates and concentrations of NO_x (the sum of NO and NO_2), CH_2O, and HO_x (the sum of OH and peroxy radicals) at 300 hPa for July 2000. Ozone production rates of up to 10 ppb day^{-1} are found over the convective regions, consistent with previous model values reported for deep convective outflow over the United States [*Pickering et al.*, 1990, 1992]. NO_x concentrations are 150–300 ppt over much of the eastern United Sates, of which lightning contributes 50–100 ppt and the rest is anthropogenic. Concentrations of HO_x radicals are as high as 10 ppt over

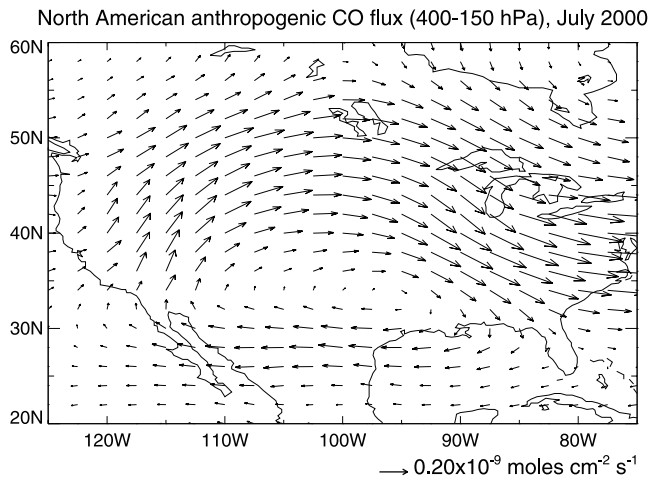

Figure 11. GEOS-CHEM monthly mean horizontal flux of North American anthropogenic CO averaged over the 400–150 hPa column for July 2000.

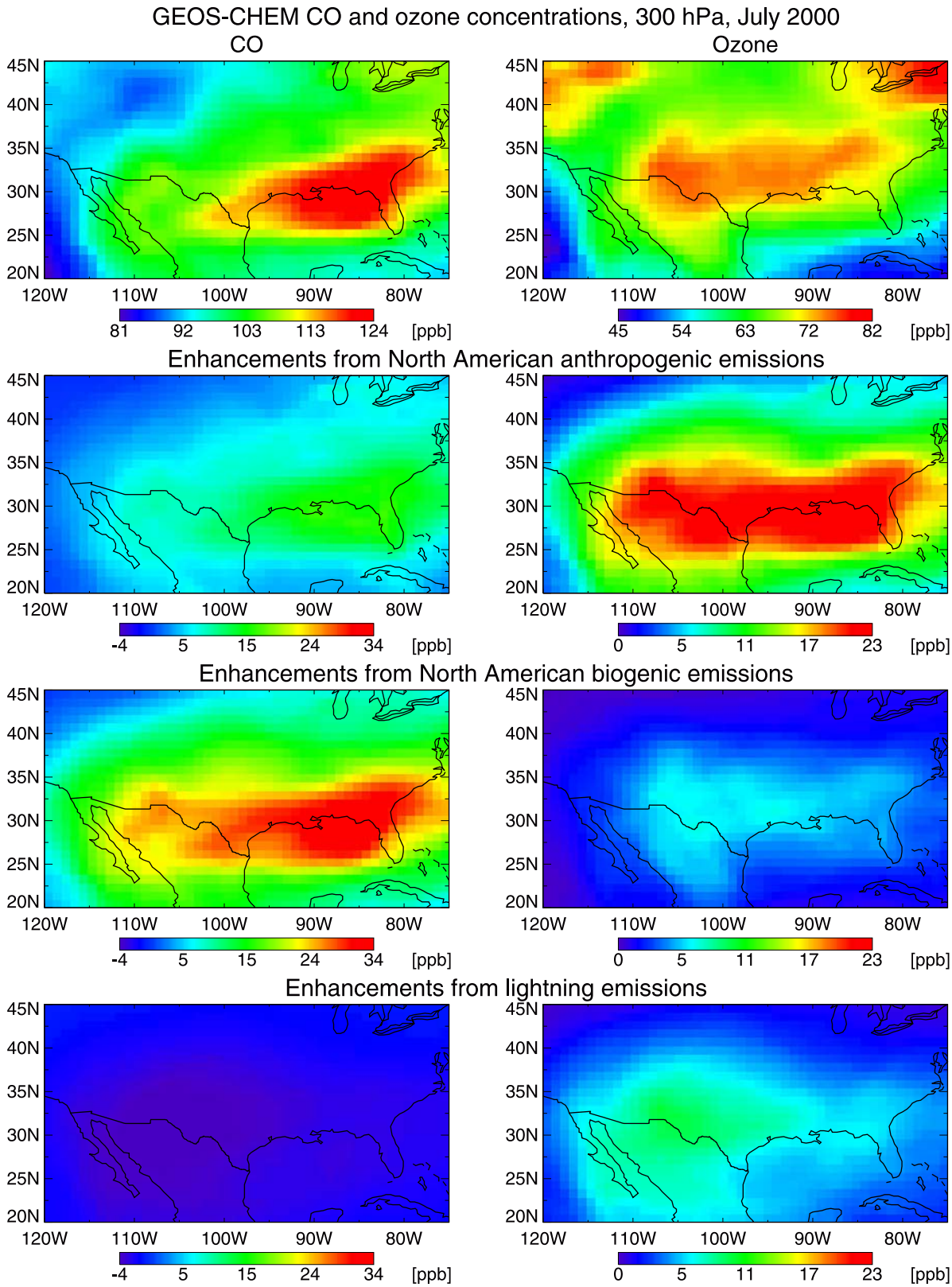

Figure 12. Simulated CO and ozone concentrations at 300 hPa for July 2000. The top shows the mean values from the standard simulation. The bottom shows the enhancements from North American anthropogenic, biogenic, and lightning emissions, as determined by difference with sensitivity simulations where these emissions are shut off separately.

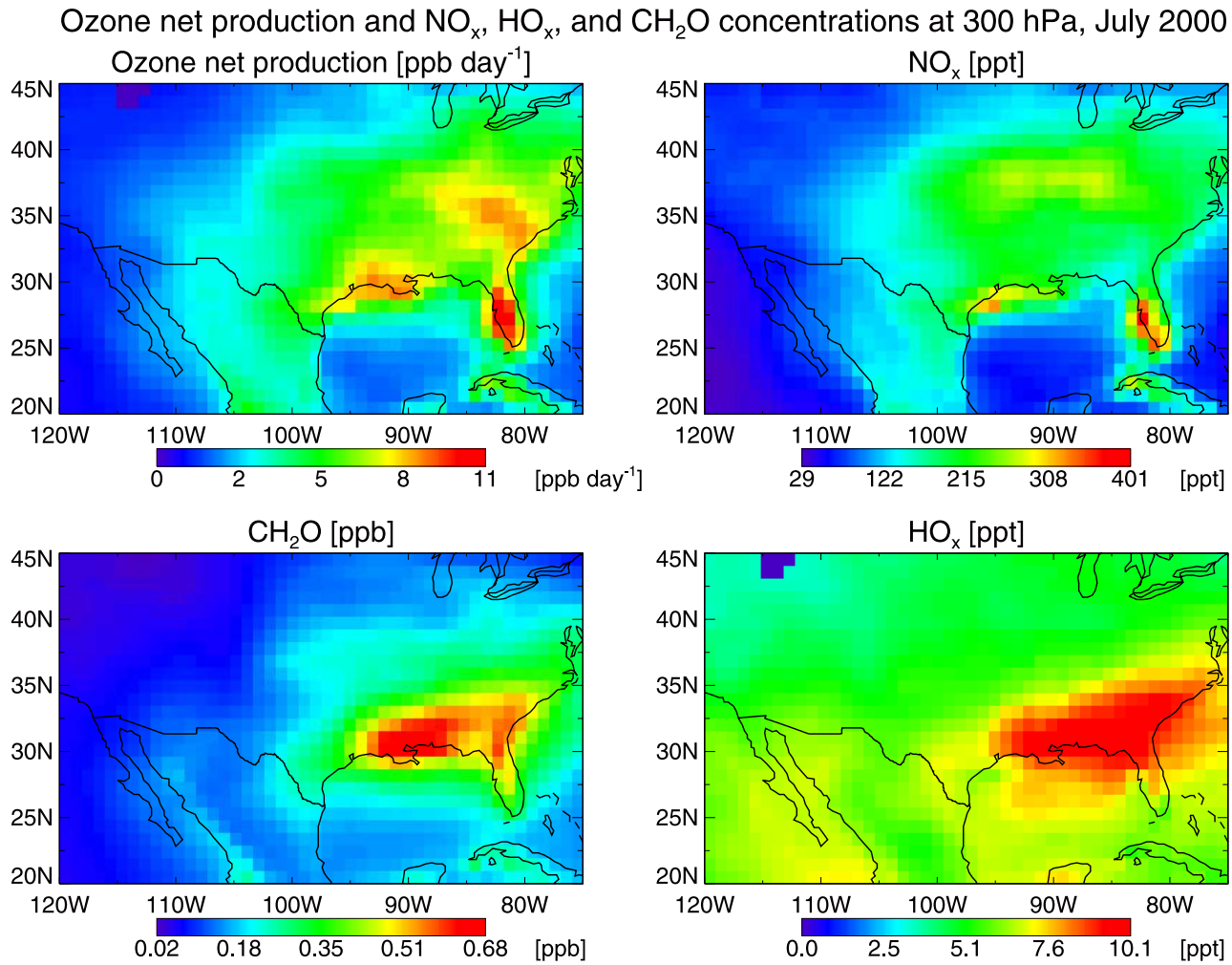

Figure 13. Simulated ozone net production and concentrations of NO_x, CH_2O, and HO_x at 300 hPa for July 2000. NO_x is the sum of NO and NO_2, and HO_x is the sum of OH and peroxy radicals.

the southeastern United States, reflecting photolysis of CH_2O originating from biogenic isoprene [*Lee et al.*, 1998; *Palmer et al.*, 2003b] and convectively pumped to the upper troposphere. Dominance of convectively lifted CH_2O as a source of the HO_x over the southeastern United States in summer has previously been suggested in a global model study by *Müller and Brasseur* [1999]. We find in the model that primary HO_x production, $P(HO_x)$ as defined by *Jaeglé et al.* [2001] exceeds 2000 ppt day^{-1} in the upper troposphere. This value of $P(HO_x)$ together with the NO_x concentrations of 150–300 imply a NO_x-limited chemical regime for ozone production in the upper troposphere [*Jaeglé et al.*, 2001]. This NO_x-limited regime is manifested in the spatial correlation of ozone production and NO_x concentration in Figure 13. Nevertheless, the coincidence of high isoprene emissions and frequent deep convection over the southeastern United States plays a major role in driving ozone production in the upper troposphere.

[30] The role of isoprene-generated CH_2O in driving ozone production in the upper troposphere becomes even larger if NO_x emissions from lightning are increased. Lightning represents the largest uncertainty among the various NO_x sources [*Price et al.*, 1997; *Nesbitt et al.*, 2000; *Tie et al.*, 2002]. Lightning NO_x emissions in GEOS-CHEM are parameterized as a function of deep convective cloud top [*Price and Rind*, 1992; *Wang et al.*, 1998] to yield a global source of 6 Tg N yr^{-1} [*Martin et al.*, 2002]. This global estimate is constrained to reproduce observed ozone and NO_y concentrations in the tropics [*Martin et al.*, 2002] but there is no effective constraint for emissions over the United States. Lightning emissions could possibly be much higher there as anthropogenic aerosols stimulate lightning activity, especially in summer [*Orville et al.*, 2001; *Steiger et al.*, 2002; *Steiger and Orville*, 2003]. In addition, process-based models for lightning NO_x generation give a range of 5–25 Tg N yr^{-1} for the global source [*Price et al.*, 1997]. We conducted a sensitivity simulation with lightning NO_x emissions over North America increased by a factor of four relative the standard simulation. Figure 14 shows the resulting net ozone production rates and concentrations of NO_x, CH_2O, and HO_x at 300 hPa for July 2000. Ozone production rates are enhanced over the convective regions with maxima reaching 12–17 ppb day^{-1}. NO_x concentrations are above 400 ppt over much of the eastern United States with maxima over major lightning source regions. HO_x concentrations decrease by 25–30% relative to the standard simulation because of losses from the NO_2 + OH and

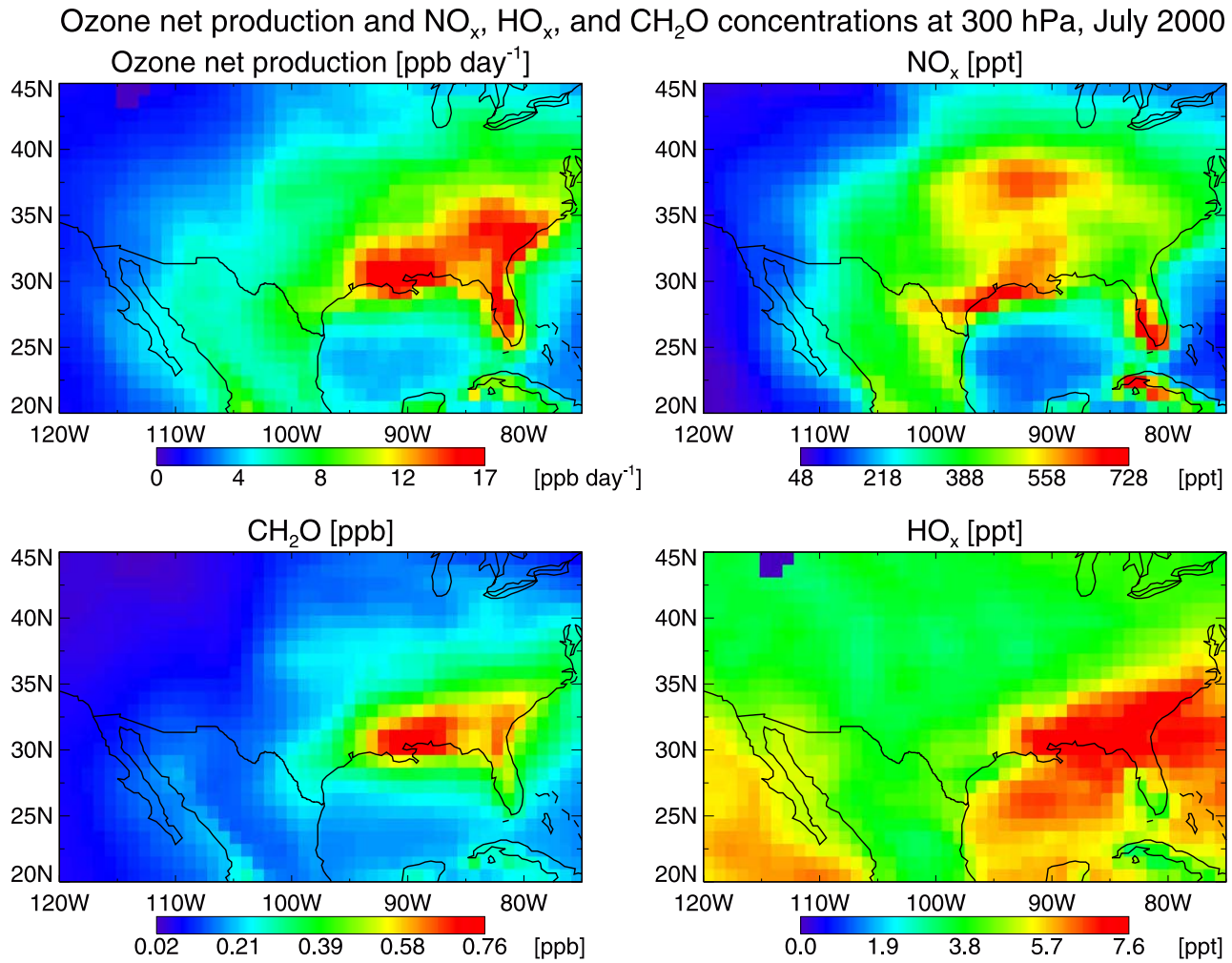

Figure 14. Same as Figure 13, but from a simulation with lightning NO_x emissions over North America increased by a factor of four from the standard simulation.

HNO_3 + OH reactions [*Jaeglé et al.*, 2001]. HO_x loss due to the HNO_x + OH reaction is less important because of the competing photolysis of HNO_x in the near infrared [*Roehl et al.*, 2002; *Salawitch et al.*, 2002]. The chemical regime for ozone production is now NO_x-saturated [*Jaeglé et al.*, 2001]. Thus the highest ozone production rates correspond to the region of highest HO_x concentrations in Figure 14. The ozone enhancement in the upper troposphere (not shown) has the same pattern as in the standard simulation, with a maximum over Texas, reflecting ozone production during the circulation around the upper-level anticyclone.

[31] There is some evidence from ozonesonde profiles for such an enhancement of ozone in the upper troposphere over the southern United States in summer. Ozonesonde profiles over Huntsville, Alabama (34.7°N, 86.5°W) show a distinct July–August enhancement in the upper troposphere above 400 hPa, with ozone concentrations over 80 ppb [*Newchurch et al.*, 2003]. This enhancement starts in late June and disappears in September, corresponding with the timing of the upper-level anticyclone (see section 4.1). Figure 15 shows the four ozonesonde profiles measured by *Newchurch et al.* [2003] over Huntsville in July 2000. Also shown are the simulated monthly ozone vertical profile from the standard simulation (with anthropogenic, biogenic, and lightning enhancements indicated) and from the simulation with lightning ×4 emissions. Ozone concentrations in the upper troposphere are over 80 ppb in the observations and about 70 ppb in the standard simulation. Increasing lightning emissions by a factor of 4 corrects the discrepancy. However, the discrepancy could also arise from a model underestimate of stratospheric influence in regions of preferential downwelling [*Hudman et al.*, 2004].

6. Summary and Conclusions

[32] We have used a global 3-D chemical transport model driven by assimilated meteorological observations (GEOS-CHEM) to examine export pathways for North American pollution to the Atlantic in summer. Simulations of CO for 4 years (1998, 2000, 2001, and 2002) with 2° × 2.5° horizontal resolution were used to examine mean outflow patterns and interannual variability. A higher-resolution (1° × 1°) simulation of tropospheric ozone-aerosol chemistry for the summer of 2000 was used to characterize the various types of outflow events and their differential impact on CO, ozone, and aerosols. We also examined the value of satellite observations of CO columns from

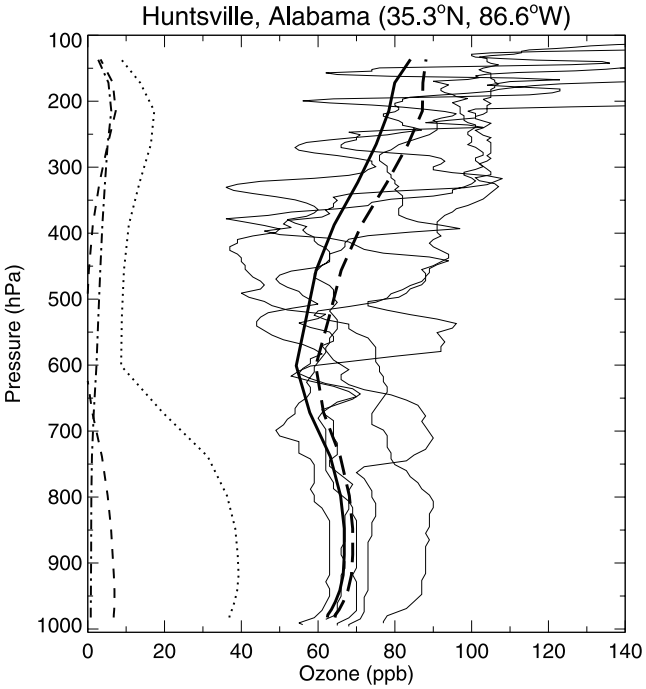

Figure 15. Vertical profiles of ozone concentrations at Huntsville, Alabama (86.6°W, 34.7°N) in July 2000. The thin solid lines are five ozonesonde soundings made during the month (1, 8, 15, 22, and 29 July) by *Newchurch et al.* [2003]. The thick solid line shows the model monthly mean values.The thin dotted, dashed, and dash-dotted lines show the simulated enhancements from North American anthropogenic, biogenic, and lightning emissions, respectively, as determined by difference with simulations where these emissions are shut off. The thick long dashes line shows the model monthly mean values from a simulation with lightning NO_x emissions over North America increased by a factor of four.

MOPITT and aerosol optical depths (AODs) from MODIS toward diagnosing North American outflow.

[33] We find that North American anthropogenic outflow to the Atlantic occurs over a broad latitude range (30–55°N), covering much of the east coast. Forest fires in Canada and the western United States are occasional contributors to the outflow. Deep convective outflow takes place preferentially over the U.S. Midwest, the Gulf Coast, and the east coast. Pollution from the West Coast is principally transported north to 45–50 N and then east, merging with the eastern U.S. pollution outflow to the Atlantic. Outflow in the boundary layer accounts for about 30% of the total export of North American CO.

[34] Outflow of North American pollution to the North Atlantic is driven principally by midlatitude cyclones that form in the lee of the Rocky Mountains and generally propagate northeastward. The frequency of North American outflow events is about 5–7 per month in summer. The associated surface cold fronts move southeastward and tend to dissipate south of 35°N. The warm conveyor belts (WCBs) associated with the cold fronts originate generally north of 30°N and extend northeastward. They lift pollution from the central and northeastern United States but usually do not reach the southeastern United States. The ascending motion in the WCBs reaches the upper troposphere over Newfoundland. Additional strong outflow takes place in the boundary layer behind the cold fronts.

[35] Deep convection plays an important role in ventilating the central and southeastern United States in summer. The semipermanent anticyclone centered in the upper troposphere over the southern United States can circulate this convective outflow over the United States for several days before eventual export to the Atlantic. Rapid ozone production (up to 10 ppb day^{-1}) takes place in the circulating outflow. This production is driven in part by anthropogenic and lightning NO_x and in part by HO_x radicals produced from convectively lifted CH_2O that originates from biogenic isoprene. It takes place near the transition between NO_x-limited and NO_x-saturated regimes for ozone production. We thus predict a large anthropogenic maximum in ozone (>80 ppbv) in the upper troposphere across the southern United States. Some evidence for this maximum is apparent in ozonesonde observations over Alabama.

[36] **Acknowledgments.** This work was performed in part at Harvard University, with support from the Office of Global Programs of the National Oceanic and Atmospheric Administration (NOAA), and at Jet Propulsion Laboratory, California Institute of Technology, under contract with the National Aeronautics and Space Administration (NASA). Discussions with Owen Cooper, Andreas Stohl, Hongyu Liu, and Jennifer Logan were very helpful.

References

Arellano, A. F., Jr., P. S. Kasibhatla, L. Giglio, G. R. van der Werf, and J. T. Randerson (2004), Top-down estimates of global CO sources using MOPITT measurements, *Geophys. Res. Lett.*, *31*, L01104, doi:10.1029/2003GL018609.

Balkanski, Y. J., D. J. Jacob, R. Arimoto, and M. A. Kritz (1992), Long-range transport of radon-222 over the North Pacific Ocean: Implications for continental influence, *J. Atmos. Chem.*, *14*, 353–374.

Bell, G. D., and L. F. Bosart (1989), A 15-year climatology of northern hemisphere 500 mb closed cyclone and anticyclone centers, *Mon. Weather Rev.*, *117*, 2142–2164.

Bey, I., D. J. Jacob, R. M. Yantosca, J. A. Logan, B. D. Field, A. M. Fiore, Q. B. Li, H. Liu, L. J. Mickley, and M. G. Schultz (2001a), Global modeling of tropospheric chemistry with assimilated meteorology: Model description and evaluation, *J. Geophys. Res.*, *106*, 23,073–23,095.

Bey, I., D. J. Jacob, J. A. Logan, and R. M. Yantosca (2001b), Asian chemical outflow to the Pacific: Origins, pathways, and budgets, *J. Geophys. Res.*, *106*, 23,097–23,113.

Browning, K. A., and G. A. Monk (1982), A simple model for the synoptic analysis of cold fronts, *Q. J. R. Meteorol. Soc.*, *108*, 435–452.

Browning, K. A., and N. M. Roberts (1994), Structure of a frontal cyclone, *Q. J. R. Meteorol. Soc.*, *120*, 1537–1557.

Carlson, T. N. (1980), Airflow through midlatitude cyclones and the comma cloud pattern, *Mon. Weather Rev.*, *108*, 1498–1509.

Carlson, T. N. (1998), *Mid-Latitude Weather Systems*, Am. Meteorol. Soc., Boston, Mass.

Chin, M., P. Ginoux, S. Kinne, O. Torres, B. Holben, B. N. Duncan, R. V. Martin, J. A. Logan, A. Higurashi, and T. Nakajima (2002), Tropospheric aerosol optical thickness from the GOCART model and comparisons with satellite and sunphotometer measurements, *J. Atmos. Sci.*, *59*, 461–483.

Chu, D. A., Y. J. Kaufman, C. Ichoku, L. A. Remer, D. Tanre, and B. N. Holben (2002), Validation of MODIS aerosol optical depth retrieval over land, *Geophys. Res. Lett.*, *29*(12), 8007, doi:10.1029/2001GL013205.

Chu, D. A., Y. J. Kaufman, G. Zibordi, J. D. Chern, J. Mao, C. Li, and B. N. Holben (2003), Global monitoring of air pollution over land from the Earth Observing System-Terra Moderate Resolution Imaging Spectroradiometer (MODIS), *J. Geophys. Res.*, *108*(D21), 4661, doi:10.1029/2002JD003179.

Cooper, O. R., J. L. Moody, D. D. Parrish, M. Trainer, J. S. Hplloway, T. B. Ryerson, G. Hubler, F. C. Fehsenfeld, S. J. Oltmans, and M. J. Evans (2001), Trace gas signatures of the airstreams within North Atlantic cyclones: Case studies from the North Atlantic Regional Experiment (NARE'97) aircraft intensive, *J. Geophys. Res.*, *106*, 5437–5456.

Cooper, O. R., J. L. Moody, D. D. Parrish, M. Trainer, J. S. Holloway, T. B. Ryerson, G. Hübler, F. C. Fehsenfeld, S. J. Oltmans, and M. J. Evans

(2002a), Trace gas composition of midlatitude cyclones over the western North Atlantic Ocean: A conceptual model, *J. Geophys. Res.*, *107*(D7), 4056, doi:10.1029/2001JD000901.

Cooper, O. R., J. L. Moody, D. D. Parrish, M. Trainer, J. S. Holloway, G. Hübler, F. C. Fehsenfeld, and A. Stohl (2002b), Trace gas composition of midlatitude cyclones over the western North Atlantic Ocean: A seasonal comparison of O_3 and CO, *J. Geophys. Res.*, *107*(D7), 4057, doi:10.1029/2001JD000902.

Deeter, M. N., et al. (2003), Operational carbon monoxide retrieval algorithm and selected results for the MOPITT instrument, *J. Geophys. Res.*, *108*(D14), 4399, doi:10.1029/2002JD003186.

Dickerson, R. R., et al. (1987), Thunderstorms - An important mechanism in the transport of air pollutants, *Science*, *235*, 460–464.

Dickerson, R. R., B. Doddridge, P. Kelley, and K. Rhoads (1995), Large scale pollution of the atmosphere over the remote Atlantic Ocean: Evidence from Bermuda, *J. Geophys. Res.*, *100*, 8945–8952.

Duncan, B. N., R. V. Martin, A. C. Staudt, R. M. Yevich, and J. A. Logan (2003), Interannual and seasonal variability of biomass burning emissions constrained by satellite observations, *J. Geophys. Res.*, *108*(D2), 4100, doi:10.1029/2002JD002378.

Eckhardt, S., and A. Stohl (2004), A 15-year climatology of warm conveyor belts, *J. Climate.*, *17*, 218–237.

Fromm, M. D., and R. Servranckx (2003), Transport of fire smoke above the tropopause by supercell convection, *Geophys. Res. Lett.*, *30*(10), 1542, doi:10.1029/2002GL016820.

Galasyn, J. F., K. L. Tschudy, and B. J. Huebert (1987), Seasonal and diurnal variability of nitric acid vapor and ionic aerosol species in the remote free troposphere at Mauna Loa, Hawaii, *J. Geophys. Res.*, *92*, 3105–3113.

Ginoux, P., M. Chin, I. Tegen, J. M. Prospero, B. Holben, O. Dubovik, and S. Lin (2001), Sources and distributions of dust aerosols simulated with GOCART model, *J. Geophys. Res.*, *106*, 3805–3818.

Heald, C. L., et al. (2003), Asian outflow and trans-Pacific transport of carbon monoxide and ozone pollution: An integrated satellite, aircraft, and model perspective, *J. Geophys. Res.*, *108*(D24), 4804, doi:10.1029/2003JD003507.

Holben, B. N., et al. (1998), AERONET - A federated instrument network and data archive for aerosol characterization, *Remote Sens. Environ.*, *66*, 1–16.

Hudman, R. C., et al. (2004), Ozone production in transpacific Asian pollution plumes and implications for ozone air quality in California, *J. Geophys. Res.*, *109*, D23S10, doi:10.1029/2004JD004974.

Intergovernmental Panel on Climate Change (IPCC) (2001), *Climate Change 2001: The Scientific Basis*, edited by J. T. Houghton et al., p. 944, Cambridge Univ. Press, New York.

Jacob, D. J., J. A. Logan, G. M. Gardner, R. M. Yevich, C. M. Spivakovsky, and S. C. Wofsy (1993), Factors regulating ozone over the United States and its export to the global atmosphere, *J. Geophys. Res.*, *98*, 14,817–14,826.

Jaeglé, L., D. J. Jacob, W. H. Brune, and P. O. Wennberg (2001), Chemistry of HO_x radicals in the upper troposphere, *Atmos. Environ.*, *35*, 469–489.

Kaufman, Y. J., D. Tanré, L. A. Remer, E. F. Vermote, A. Chu, and B. N. Holben (1997), Operational remote sensing of tropospheric aerosol over the land from EOS-MODIS, *J. Geophys. Res.*, *102*, 17,051–17,067.

Lamarque, J.-F., et al. (2003), Identification of CO plumes from MOPITT data: Application to the August 2000 Idaho-Montana forest fires, *Geophys. Res. Lett.*, *30*(13), 1688, doi:10.1029/2003GL017503.

Lee, Y. N., et al. (1998), Atmospheric chemistry and distribution of formaldehyde and several multioxygenated carbonyl compounds during the 1995 Nashville Middle Tennessee Ozone Study, *J. Geophys. Res.*, *103*(D17), 22,449–22,462.

Li, Q. B., et al. (2001), A tropospheric ozone maximum over the Middle East, *Geophys. Res. Lett.*, *28*, 3235–3238.

Li, Q. B., et al. (2002a), Transatlantic transport of pollution and its effects on surface ozone in Europe and North America, *J. Geophys. Res.*, *107*(D13), 4166, doi:10.1029/2001JD001422.

Li, Q. B., D. J. Jacob, T. D. Fairlie, H. Liu, R. M. Yantosca, and R. V. Martin (2002b), Stratospheric versus pollution influences on ozone at Bermuda: Reconciling past analyses, *J. Geophys. Res.*, *107*(D22), 4611, doi:10.1029/2002JD002138.

Li, Q. B., D. J. Jacob, R. M. Yantosca, J. W. Munger, and D. D. Parrish (2004), Export of NO_y from the North American boundary layer: Reconciling aircraft observations and global model budgets, *J. Geophys. Res.*, *109*, D02313, doi:10.1029/2003JD004086.

Liu, H., D. J. Jacob, I. Bey, and R. M. Yantosca (2001), Constrains from ^{210}Pb and ^{7}Be on wet deposition and transport in a global three-dimensional chemical tracer model driven by assimilated meteorological fields, *J. Geophys. Res.*, *106*, 12,109–12,128.

Liu, H., D. J. Jacob, I. Bey, R. M. Yantosca, and B. N. Duncan (2003), Transport pathways for Asian outflow over the Pacific: Interannual and seasonal variations, *J. Geophys. Res.*, *108*(D20), 8786, doi:10.1029/2002JD003102.

Logan, J. A. (1989), Ozone in rural-areas of the United States, *J. Geophys. Res.*, *94*(D6), 8511–8532.

Maddox, R. A. (1980), Mesoscale convective complexes, *Bull. Am. Meteorol. Soc.*, *61*, 1374–1387.

Martin, R. V., et al. (2002), Interpretation of TOMS observations of tropical tropospheric ozone with a global model and in situ observations, *J. Geophys. Res.*, *107*(D18), 4351, doi:10.1029/2001JD001480.

Martin, R. V., D. J. Jacob, R. M. Yantosca, M. Chin, and P. Ginoux (2003), Global and regional decreases in tropospheric oxidants from photochemical effects of aerosols, *J. Geophys. Res.*, *108*(D3), 4097, doi:10.1029/2002JD002622.

Merrill, J. T., and J. L. Moody (1996), Synoptic meteorology and transport during the North Atlantic Regional Experiment (NARE) intensive: Overview, *J. Geophys. Res.*, *101*, 28,903–28,921.

Moody, J. L., J. C. Davenport, J. T. Merrill, S. J. Oltmans, D. D. Parrish, J. S. Holloway, H. Levy II, G. L. Forbes, M. Trainer, and M. Buhr (1996), Meteorological mechanisms for transporting O_3 over the western North Atlantic Ocean: A case study for August 24–29, 1993, *J. Geophys. Res.*, *101*, 29,213–29,227.

Moxim, W. J. (1990), Simulated transport of NO_y to Hawaii during August—A synoptic study, *J. Geophys. Res.*, *95*, 5717–5729.

Müller, J.-F., and G. Brasseur (1999), Sources of upper tropospheric HO_x: A three-dimensional study, *J. Geophys. Res.*, *104*, 1705–1715.

Nesbitt, S. W., R. Y. Zhang, and R. E. Orville (2000), Seasonal and global NO_x production by lightning estimated from the Optical Transient Detector (OTD), *Tellus, Ser. B*, *52*, 1206–1215.

Newchurch, M. J., M. A. Ayoub, S. Oltmans, B. Johnson, and F. J. Schmidlin (2003), Vertical distribution of ozone at four sites in the United States, *J. Geophys. Res.*, *108*(D1), 4031, doi:10.1029/2002JD002059.

Orville, R. E., G. Huffines, J. Nielsen-Gammon, R. Y. Zhang, B. Ely, S. Steiger, S. Phillips, S. Allen, and W. Read (2001), Enhancement of cloud-to-ground lightning over Houston, Texas, *Geophys. Res. Lett.*, *28*, 2597–2600.

Palmer, P. I., D. J. Jacob, D. B. A. Jones, C. L. Heald, B. M. Yantosca, J. A. Logan, G. W. Sachse, and D. G. Streets (2003a), Inverting for emissions of carbon monoxide from Asia using aircraft observations over the western Pacific, *J. Geophys. Res.*, *108*(D21), 8825, doi:10.1029/2002JD003176.

Palmer, P. I., D. J. Jacob, A. M. Fiore, R. V. Martin, K. Chance, and T. P. Kurosu (2003b), Mapping isoprene emissions over North America using formaldehyde column observations from space, *J. Geophys. Res.*, *108*(D6), 4180, doi:10.1029/2002JD002153.

Park, R. J., D. J. Jacob, M. Chin, and R. V. Martin (2003), Sources of carbonaceous aerosols over the United States and implications for natural visibility, *J. Geophys. Res.*, *108*(D12), 4355, doi:10.1029/2002JD003190.

Park, R. J., D. J. Jacob, B. D. Field, R. M. Yantosca, and M. Chin (2004), Natural and transboundary pollution influences on sulfate-nitrate-ammonium aerosols in the United States: Implications for policy, *J. Geophys. Res.*, *109*, D15204, doi:10.1029/2003JD004473.

Parker, S. S., J. T. Hawes, S. J. Colucci, and B. P. Hayden (1989), Climatology of 500 mb cyclones and anticyclones, 1950–1985, *Mon. Weather Rev.*, *117*, 558–571.

Parrish, D. D., M. Trainer, D. Hereid, E. J. Williams, K. J. Olszyna, R. A. Harley, J. F. Meagher, and F. C. Fehsenfeld (2002), Decadal change in carbon monoxide to nigrogen oxide ratio in U.S. vehicular emissions, *J. Geophys. Res.*, *107*(D12), 4140, doi:10.1029/2001JD000720.

Pickering, K. E., R. R. Dickerson, G. J. Huffman, J. F. Boatman, and A. Schanot (1988), Trace gase transport in the vicinity of frontal convective clouds, *J. Geophys. Res.*, *93*, 759–773.

Pickering, K. E., A. M. Thompson, R. R. Dickerson, W. T. Luke, D. P. McNamara, J. P. Greenberg, and P. R. Zimmerman (1990), Model calculations of tropospheric ozone production potential following observed convective events, *J. Geophys. Res.*, *95*, 14,049–14,062.

Pickering, K. E., A. M. Thompson, J. R. Scala, W.-K. Tao, R. R. Dickerson, and J. Simpson (1992), Free tropospheric ozone production following entrainment of urban plumes into deep convection, *J. Geophys. Res.*, *97*, 17,985–18,000.

Price, C., and D. Rind (1992), A simple lightning parameterization for calculating global lightning distributions, *J. Geophys. Res.*, *97*, 9919–9933.

Price, C., J. Penner, and M. Prather (1997), NO_x from lightning: 1. Global distribution based on lightning physics, *J. Geophys. Res.*, *102*, 5929–5941.

Remer, L. A., et al. (2002), Validation of MODIS aerosol retrieval over ocean, *Geophys. Res. Lett.*, *29*(12), 8008, doi:10.1029/2001GL013204.

Roehl, C. M., S. A. Nizkorodov, H. Zhang, G. A. Blake, and P. O. Wennberg (2002), Photodissociation of peroxynitric acid in the near-IR, *J. Phys. Chem. A*, *106*(15), 3766–3772, doi:10.1021/jp013536v.

Salawitch, R. J., P. O. Wennberg, G. C. Toon, B. Sen, and J. F. Blavier (2002), Near IR photolysis of HO_2NO_2: Implications for HO_x, *Geophys. Res. Lett.*, *29*(D16), 1762, doi:10.1029/2002GL015006.

Staudt, A. C., D. J. Jacob, J. A. Logan, D. Bachiochi, T. N. Krishnamurti, and G. W. Sachse (2001), Continental sources, transoceanic transport, and interhemispheric exchange of carbon monoxide over the Pacific, *J. Geophys. Res.*, *106*, 32,571–32,589.

Steiger, S. M., and R. E. Orville (2003), Cloud-to-ground lightning enhancement over southern Louisiana, *Geophys. Res. Lett.*, *30*(19), 1975, doi:10.1029/2003GL017923.

Steiger, S. M., R. E. Orville, and G. Huffines (2002), Cloud-to-ground lightning characteristics over Houston, Texas: 1989–2000, *J. Geophys. Res.*, *107*(D11), 4117, doi:10.1029/2001JD001142.

Stohl, A. (2001), A 1-year Lagrangian "climatology" of airstreams in the Northern Hemisphere troposphere and lowermost stratosphere, *J. Geophys. Res.*, *106*, 7263–7279.

Tanré, D., Y. J. Kaufman, M. Herman, and S. Mattoo (1997), Remote sensing of aerosol properties over oceans using the MODIS/EOS spectral radiances, *J. Geophys. Res.*, *102*, 16,971–16,988.

Thompson, A. M., K. E. Pickering, R. R. Dickerson, W. G. Ellis Jr., D. J. Jacob, J. R. Scala, W.-K. Tao, D. P. McNamara, and J. Simpson (1994), Convective transport over the central United States and its role in regional CO and ozone budgets, *J. Geophys. Res.*, *99*, 18,703–18,711.

Tie, X. X., R. Y. Zhang, G. Brasseur, and W. F. Lei (2002), Global NO_x production by lightning, *J. Atmos. Chem.*, *43*(1), 61–74.

United States Environmental Protection Agency (2000), National air quality and emission trends, 1998, Washington, D. C.

Wang, Y., D. J. Jacob, and J. A. Logan (1998), Global simulation of tropospheric O_3-NO_x-hydrocarbon chemistry: 1. Model formulation, *J. Geophys. Res.*, *103*, 10,713–10,725.

Wang, Y. X., M. B. McElroy, D. J. Jacob, and R. M. Yantosca (2004), A nested grid formation for chemical transport over Asia: Applications to CO, *J. Geophys. Res.*, *109*, D22307, doi:10.1029/2004JD005237.

Whelpdale, D. M., T. B. Low, and R. J. Kolomeychuk (1984), Advection climatology for the east coast of North America, *Atmos. Environ.*, *18*, 1311–1327.

Whittaker, K. M., and L. H. Horn (1984), Northern hemisphere extratropical cyclone activity for four mid-season months, *J. Climatol.*, *4*, 297–310.

Wotawa, G., and M. Trainer (2000), The influence of Canadian forest fires on pollutant concentrations in the United States, *Science*, *288*, 324–328.

Zishka, K. M., and P. J. Smith (1980), The climatology of cyclones and anticyclones over North America and surrounding ocean environs for January and July, 1950–1977, *Mon. Weather Rev.*, *108*, 387–401.

M. Evans, School of the Environment, University of Leeds, Leeds LS2 0TJ, UK.

C. L. Heald, R. Hudman, D. J. Jacob, R. Park, Y. Wang, and R. M. Yantosca, Department of Earth and Planetary Sciences, Division of Engineering and Applied Sciences, Harvard University, Cambridge, MA 02138, USA.

Q. Li, Jet Propulsion Laboratory, California Institute of Technology, 4800 Oak Grove Drive, M/S 183-501, Pasadena, CA 91109, USA. (qinbin.li@jpl.nasa.gov)

R. V. Martin, Department of Physics and Atmospheric Science, Dalhousie University, Halifax, Nova Scotia B3H 3J5, Canada.